

Rampant changes in $5f_{5/2}$ and $5f_{7/2}$ filling across the light and middle actinide metals: Electron energy-loss spectroscopy, many-electron atomic spectral calculations, and spin-orbit sum rule

K. T. Moore,^{1,*} G. van der Laan,² M. A. Wall,¹ A. J. Schwartz,¹ and R. G. Haire³

¹Lawrence Livermore National Laboratory, Livermore, California 94550, USA

²Magnetic Spectroscopy Group, Daresbury Laboratory, Warrington WA4 4AD, United Kingdom

³Oak Ridge National Laboratory, MS-6375, Oak Ridge, Tennessee 37831, USA

(Received 8 May 2007; published 23 August 2007)

We examine the branching ratio of the $N_{4,5}$ ($4d \rightarrow 5f$) spectra of Th, U, Np, Pu, Am, and Cm metals using electron energy-loss spectroscopy (EELS) in a transmission electron microscope, together with many-electron atomic spectral calculations and the spin-orbit sum rule. Our results show the following. (1) The actinide metals Pu, Am, and Cm exhibit intermediate coupling. (2) The intermediate coupling values for the $5f$ states as calculated using a many-electron atomic model are correct for the actinides; this being proven by our results for curium. (3) The EELS branching ratio is sensitive to the degree of $5f$ electron delocalization, which is illustrated by the transition from LS to intermediate coupling between U and Pu.

DOI: [10.1103/PhysRevB.76.073105](https://doi.org/10.1103/PhysRevB.76.073105)

PACS number(s): 71.27.+a, 71.10.-w, 71.20.Gj, 79.20.Uv

Actinide materials are rapidly growing in importance for energy and industry, particularly given the exploding interest in next-generation nuclear reactors. Yet despite this rising awareness, there is a gaping lack in the general knowledge of the fundamental physics and materials science of many of these materials, even for the elemental metals. For accurate modeling of the behavior of these materials, a better understanding of the basic aspects of actinide metals, alloys, and materials is required through experiment and theory. Considerable strides to increase this understanding have indeed been achieved,¹⁻⁸ but many questions remain. A particularly fundamental question is how the $5f$ electrons fill the $j=5/2$ and $7/2$ levels across the series, i.e., the type of angular-momentum coupling that each actinide exhibits.^{9,10} To this end, we are systematically investigating the $5f$ states of the elemental actinide metals, since these are the states governing much of the unique electron bonding and physical properties.

The $5f$ states of actinide materials can be directly examined via electron energy-loss spectroscopy (EELS) or x-ray absorption spectroscopy. With either technique, a core electron is excited above the Fermi energy, directly probing the unoccupied states. Using excitations from a d core level, the $5f$ spin-orbit interaction per hole can be directly examined for a particular actinide material by the spin-orbit sum rule.⁹⁻¹² For this analysis, the branching ratio must be extracted from the spin-orbit-split core-level edges in the spectra, which in our case is gathered from the $N_{4,5}$ ($4d \rightarrow 5f$) edges. Electric-dipole selection rules allow two kinds of transitions: N_5 ($4d_{5/2} \rightarrow 5f_{5/2,7/2}$) and N_4 ($4d_{3/2} \rightarrow 5f_{5/2}$). Since an electron from a d core state can only be excited into specific $5f$ states, this leads to differences in the branching ratio that can be interrogated using the spin-orbit sum rule.

In this Brief Report, we employ EELS in a transmission electron microscope (TEM), combined with many-electron atomic calculations and the spin-orbit sum rule to examine the electronic structure of the $5f$ states in the ground-state phase of Th, U, Np, Pu, Am, and Cm metal by means of the $N_{4,5}$ transition.¹³ The spectra of Th, U, and Pu were shown

previously,^{9,10} but here different spectra for Np, Am, and Cm are given. The branching ratio of the $N_{4,5}$ EELS spectra, and in turn the spin-orbit sum rule analysis, reveals that while the light actinide U exhibits LS coupling, the middle actinides Pu, Am, and Cm exhibit intermediate coupling. Data for Cm show a large shift in the angular-momentum coupling mechanism toward the LS limit, a fact that solidifies that the spin-orbit sum rule is indeed accurate in describing the $5f$ states. Further, the experimental EELS data for Pu, Am, and Cm fit the intermediate coupling model exceedingly well, thus supporting that the valence for each metal is at, or near, 5, 6, and 7, respectively. Finally, the data also show that the branching ratio is sensitive to delocalization. This is illustrated in the transition from LS to intermediate coupling between U and Pu, with Np falling in the middle of the two curves. Pertaining to methods of experiment and theory, EELS experiments in the TEM^{9,10} and atomic calculations^{11,12} were performed in a manner similar to the references cited.

The $N_{4,5}$ edge for each metal is shown in Fig. 1, where each spectrum is normalized to the N_5 ($4d_{5/2}$) peak height. Immediately noticeable is the gradually growing separation between the N_4 and N_5 peaks from Th to Cm, in pace with the increase in $4d$ spin-orbit splitting with atomic number. Also noticeable is that the N_4 ($4d_{3/2}$) peak reduces in intensity going from Th to Am, but then the trend reverses, giving a larger intensity for Cm. The behavior of the N_4 peak in the EELS spectra in Fig. 1 directly reflects the filling of the angular-momentum levels in the $5f$ state. Selection rules govern that a $d_{3/2}$ electron can only be excited into an empty $f_{5/2}$ level, which means that the ratio of the N_4 ($d_{3/2}$) and N_5 ($d_{5/2}$) peak intensities serves as a measure for the relative occupation of the $5f_{5/2}$ and $5f_{7/2}$ levels. The N_4 peak reduces rapidly as the atomic number increases because the majority of the $5f$ electrons are occupying the $f_{5/2}$ level. By the time Am is reached, the N_4 peak is almost extinct since the $f_{5/2}$ level is close to full with six $5f$ electrons (there is only a minor amount of electrons in the $f_{7/2}$ level). Thus, there is little room for an electron from $d_{3/2}$ to be excited into the

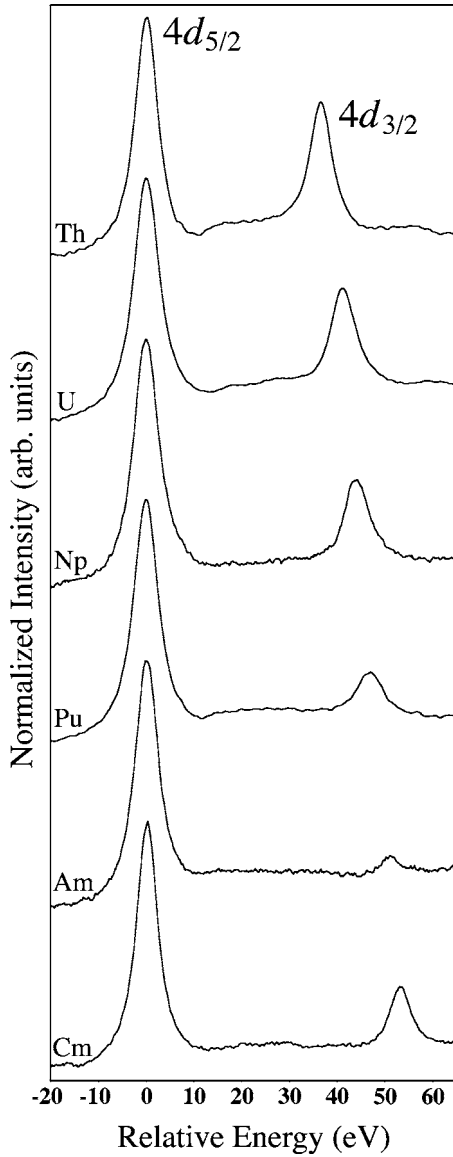


FIG. 1. The $N_{4,5}$ EELS spectra for Th, U, Np, Pu, Am, and Cm metals, each normalized to the N_5 peak height. Note that the N_4 ($4d_{5/2}$) edge gradually decreases in intensity relative to the N_5 ($4d_{3/2}$) edge going from Th to Am, then increases again for Cm.

$5f_{7/2}$ level. For Cm, the N_4 peak then increases relative to the N_5 peak for particular reasons discussed below.

For the f shell, the number of electrons n_f and the expectation value of the angular part of the spin-orbit interaction $\langle w^{110} \rangle$ is given as

$$n_f = n_{7/2} + n_{5/2}, \quad (1)$$

$$\langle w^{110} \rangle \equiv \frac{2}{3} \langle l \cdot s \rangle = n_{7/2} - \frac{4}{3} n_{5/2}, \quad (2)$$

where $n_{7/2}$ and $n_{5/2}$ are the electron occupation numbers of the angular-momentum levels $j=7/2$ and $5/2$.⁹⁻¹² Thus, $\langle w^{110} \rangle$ reveals the proper angular-momentum coupling scheme for a given material. The branching ratio

TABLE I. The expected number of $5f$ electrons n_f , the experimental branching ratio B of the $N_{4,5}$ EELS spectra, and the expectation value of the $5f$ spin-orbit interaction per hole $\langle w^{110} \rangle / (14 - n_f) - \Delta$ obtained using Eq. (3) for the α phase of Th, U, Np, Pu, Am, and Cm metals. Each branching ratio value is an average of between 10 and 20 EELS spectra, with the standard deviation given in parentheses. The sum rule requires a small correction factor, which is $\Delta = -0.017, -0.010, -0.005, 0.000, 0.005,$ and 0.015 for $n_f = 1, 3, 4, 5, 6,$ and 7 , respectively. The experimental electron occupation numbers $n_{5/2}$ and $n_{7/2}$ of the $f_{5/2}$ and $f_{7/2}$ levels are obtained by solving Eqs. (1) and (2).

Metal	n_f	B	$\langle w^{110} \rangle / (14 - n_f) - \Delta$	$n_{5/2}$	$n_{7/2}$
Th	1.3	0.646 (003)	-0.115 (008)	1.28	0.02
U	3	0.686 (002)	-0.215 (005)	2.35	0.65
Np	4	0.740 (005)	-0.350 (013)	3.24	0.76
Pu	5	0.826 (010)	-0.565 (025)	4.32	0.68
Am	6	0.930 (005)	-0.825 (013)	5.38	0.62
Cm	7	0.794 (003)	-0.485 (008)	4.41	2.59

$B = I(N_5) / [I(N_5) + I(N_4)]$ is obtained by calculating the second derivative of the raw EELS spectra, and then integrating the area beneath the N_5 and N_4 peaks above zero, which yields the integrated intensities $I(N_5)$ and $I(N_4)$. The experimental branching ratios for Th, U, Np, Pu, Am, and Cm metals are listed in Table I. For each metal, the value of the branching ratio is fed into the spin-orbit sum rule, yielding the spin-orbit interaction per hole.¹² For the $d \rightarrow f$ transition, the sum rule is given as

$$\frac{\langle w^{110} \rangle}{14 - n_f} - \Delta = -\frac{5}{2} \left(B - \frac{3}{5} \right), \quad (3)$$

where Δ represents a small correction term for the sum rule calculated using Cowan's relativistic Hartree-Fock code.^{9,14} Table I lists the spin-orbit interaction per hole and the correction factor for each actinide metal.

In order to visualize the spin-orbit analysis of the EELS spectra in relation to our atomic calculations, both are shown on a plot of $\langle w^{110} \rangle / (14 - n_f) - \Delta$ as a function of the number of f electrons in Fig. 2(a). The curves for the three theoretical angular-momentum coupling schemes, LS , jj , and intermediate, as calculated using a many-electron atomic model, are plotted as short-dashed, long-dashed, and solid lines, respectively. The experimental EELS results are indicated by points. Th metal falls close to all three curves, which is due to the fact that it takes two electrons to tangle, and with barely more than one $5f$ electron in Th there is little difference between the coupling mechanisms. A $5f$ electron count of 1.3 for Th is higher than previous experimental findings,^{1,9,10} but this is the lowest value that does not yield a negative $j=7/2$ occupation, which would be unphysical. The f count itself is not a direct output of the experiment and the uncertainty can be large if B is close to $2/3$. The different result may be due to how the second-derivative peak integration technique handles the rather peculiar background between the N_4 and N_5 peak in Th. Previous branching ratio results for Th^{9,10} were extracted using peak fitting of the

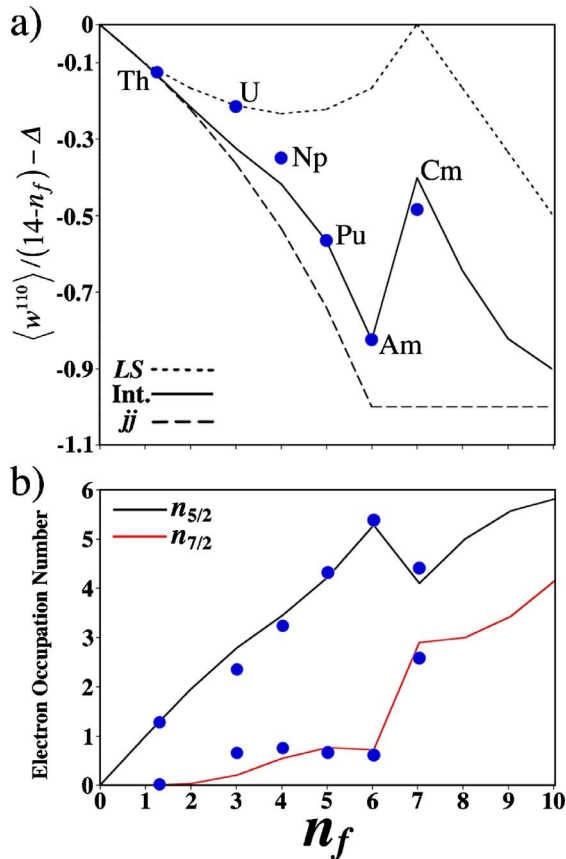


FIG. 2. (Color online) (a) Ground-state spin-orbit interaction per hole, $\langle w^{110} \rangle / (14 - n_f) - \Delta$, as a function of the number of 5f electrons (n_f). The three theoretical angular-momentum coupling schemes are shown: *LS*, *jj*, and intermediate. The points indicate the results of the spin-orbit analysis using the experimentally measured branching ratios of each metal in Fig. 1. (b) Electron occupation numbers $n_{5/2}$ and $n_{7/2}$ calculated in intermediate coupling as a function of n_f . The points indicate the experimental results: the ground-state $n_{5/2}$ and $n_{7/2}$ occupation numbers of the 5f shell from the spin-orbit analysis of the EELS spectra in Fig. 1.

EELS peaks and suggested an f count of 0.6.

Uranium falls directly on the *LS* coupling curve, Np falls between the *LS* and intermediate curve, and Pu, Am, and Cm all fall on or near the intermediate coupling curve. The intermediate curve is strongly shifted toward the *jj* limit for Pu and Am, evidencing the strong preference of the 5f electrons for the $5f_{5/2}$ level in these two metals.^{9,10,15,16} However, at Cm there is a sudden and pronounced shift in the intermediate coupling curve toward the *LS* limit.

We can calculate the electron occupation numbers $n_{7/2}$ and $n_{5/2}$ by substituting the values of n_f and $\langle w^{110} \rangle$ in Eqs. (1) and (2). The experimental and theoretical results are listed in Table I and displayed in Fig. 2(b), where the number of electrons in the $5f_{5/2}$ and $5f_{7/2}$ levels as calculated in intermediate coupling using the atomic model is drawn with lines. Again, the experimental EELS results are indicated with points. Apart from the slight deviation in the lighter actinides, U and Np, which is caused by delocalization of the 5f states and thus indicates a departure from the atomic

model, the EELS results are in excellent agreement with the theoretical curves. Figure 2(b) clearly shows that for the actinide metals up to and including Am, the 5f electrons strongly prefer the $5f_{5/2}$ level. However, this changes in a striking manner at Cm, where not only does the electron occupation sharply increase for the $5f_{7/2}$ level but even decreases for the $5f_{5/2}$ level. The results shown in Figs. 1 and 2 lead to several conclusions, each of which will be addressed.

The spin-orbit sum rule is sensitive to the degree of delocalization. This was previously alluded to in Ref. 9, but here it is solidified by the Np results. The early actinide metals, particularly U, exhibit *LS* coupling. However, the middle actinide metals Pu, Am, and Cm adhere to intermediate coupling. Most interesting is the transition that occurs between U and Pu, where the EELS results change from a pure *LS* coupling for U to a pure intermediate coupling for Pu with Np falling in between these curves (slightly biased toward intermediate coupling). This shows that the branching ratio is sensitive to the degree of delocalization of the 5f states. An *LS* mechanism is clearly observed in the more delocalized U metal, but as the 5f states become progressively more localized the coupling mechanism shifts toward intermediate coupling, being directly on the intermediate coupling curve by Pu.

These results illustrate that Pu metal is not quite as delocalized as previously believed. In solids with localized states, a pure intermediate coupling mechanism would be expected, and this is exactly what α -Pu metal exhibits in Figs. 1 and 2. This is, in fact, true for both α - and δ -Pu, since previous branching ratio and spin-orbit sum rule analysis revealed only a minor difference between the two phases.¹⁵ Thus, while the spin-orbit sum rule is sensitive to the degree of delocalization between each individual element, any change in localization between α - and δ -Pu is near the limit of detectability with the present technique.

Intermediate coupling for the 5f states as obtained from atomic calculations is the appropriate scheme for Pu, Am, and Cm. Although the early actinide metals deviate from the intermediate coupling curve due to delocalization, Fig. 2(a) shows that the middle actinide metals fall directly on it. Once the metals adopt intermediate coupling (from Pu to Cm), the curve in Fig. 2(a) is exceedingly accurate and this is clearly proven by the results for curium. Pu and Am exhibit intermediate coupling that is strongly shifted toward the *jj* limit. In *jj* coupling, the electrons first fill the $f_{5/2}$ level, which can hold no more than six, and then begin to fill the $f_{7/2}$ level. This means that in *jj* coupling the maximal energy gain due to spin-orbit interaction is obtained for Am f^6 , where the $f_{5/2}$ level is full. For Cm f^7 , at least one electron must occupy the $f_{7/2}$ level. The f^7 configuration obtains maximal energy stabilization due to exchange interaction, with all spins parallel in the half-filled shell, and this can only be achieved in *LS* coupling. Thus, the intermediate curve is strongly shifted toward the *LS* limit, as seen in Fig. 2(a), to accommodate Hund's first rule. For Pu, Am, and Cm, the spin orbit and exchange interaction compete with each other, resulting in intermediate coupling, and this is why Am f^6 still exhibits a very small N_4 peak in the EELS spectrum. However, increasing n_f from 6 to 7, a clear and pronounced shift from optimal spin-orbit stabilization for f^6 to optimal exchange interaction

stabilization for f^7 is observed. Accordingly, the N_4 peak in the Cm EELS spectrum becomes once again larger, similar to the actinide metals prior to Am. The change in electron occupation number at Cm is, in fact, so strong that, compared to Am, not one but two electrons are transferred to the $f_{7/2}$ level in Cm, as seen in Table I and Fig. 2(b). This large change in the $5f$ electron occupation numbers of the angular-momentum states directly influences the magnitude of the magnetic moment exhibited by Cm, and this in turn affects the crystal structure of the metal.¹⁷

Pu, Am, and Cm metal are near $5f^5$, $5f^6$, and $5f^7$, respectively. While the number of $5f$ electrons is not an output of our EELS and spin-orbit analysis, the results in Figs. 1 and 2 for Pu, Am, and Cm metals clearly show that the $5f$ count is at or near 5, 6, and 7, respectively. This is directly attributed to how well the EELS data track the intermediate coupling curve for these metals and exhibit the large change in angular-momentum state occupancy between Am and Cm. In the case of Pu, it has recently been shown using dynamical mean field theory¹⁸ that the $5f$ count is 5.2, which the authors derive using the branching ratio of the calculated $N_{4,5}$ x-ray absorption spectrum. In addition, experimental and theoretical data^{9,10,15–17,19} indicate an f count at or near 5 for Pu. This begs the question if Pu is $5f^5$, why then is there no experimentally observed magnetism in any of the six allotropic phases of the metal?²⁰ The lack of magnetism for Am is obvious, since it has a nearly filled $j=5/2$ level (total angular momentum $J=0$), but Pu, which is f^5 and has at least

one hole in the $j=5/2$ level, is vexing. Some mechanism—Kondo shielding, pairing correlations, etc.—must be obfuscating the moment that should be produced by the hole in the $j=5/2$ level of Pu. Indeed, recent magnetic susceptibility measurements have shown that localized magnetic moments on the order of $0.05\mu_B/\text{atom}$ form in Pu as damage accumulates due to self-irradiation.²¹ This suggests that small perturbations to the gentle balance of electronic and magnetic structure of Pu metal may destroy or degrade possible screening effects of a moment due to the hole in the $j=5/2$ level. If indeed the Kondo shielding picture is correct, then Pu has most of the spectral weight in the Hubbard bands with a small Kondo peak, which is, in fact, observed in experiments.⁴ This configuration makes Pu appear localized-like at high frequencies when probed by EELS because the technique examines the integral of the valence density of states. However, itinerant quasiparticles coexist with the atomiclike Hubbard bands and this allows Pu metal to vary density through its allotropic phases.

Finally, our EELS results show an f count of 6 for Am metal, as seen previously,^{22,23} and an f count of 7 for Cm, as supported by experiment^{6,17} and theory.¹⁸

This work was performed under the auspices of U.S. DOE by the University of California, LLNL under Contract No. W-7405-Eng-48 and by DE-AC05-00OR22725 with ORNL, operated by UT-Battelle.

*Author to whom correspondence should be addressed. FAX: 925-422-6892; moore78@llnl.gov

¹Y. Baer and J. K. Lang, Phys. Rev. B **21**, 2060 (1980).

²G. H. Lander, E. S. Fisher, and S. D. Bader, Adv. Phys. **43**, 1 (1994).

³S. Y. Savrasov and G. Kotliar, Phys. Rev. Lett. **84**, 3670 (2000).

⁴L. Havela, T. Gouder, F. Wastin, and J. Rebizant, Phys. Rev. B **65**, 235118 (2002).

⁵J. Wong, M. Krisch, D. L. Farber, F. Occelli, A. J. Schwartz, T.-C. Chiang, M. Wall, C. Boro, and R. Xu, Science **301**, 1080 (2003).

⁶S. Heathman, R. G. Haire, T. Le Bihan, A. Lindbaum, M. Idiri, P. Normile, S. Li, R. Ahuja, B. Johansson, and G. H. Lander, Science **309**, 110 (2005).

⁷K. T. Moore, P. Söderlind, A. J. Schwartz, and D. E. Laughlin, Phys. Rev. Lett. **96**, 206402 (2006).

⁸M. E. Manley, M. Yethiraj, H. Sinn, H. M. Volz, A. Alatas, J. C. Lashley, W. L. Hulst, G. H. Lander, and J. L. Smith, Phys. Rev. Lett. **96**, 125501 (2006).

⁹G. van der Laan, K. T. Moore, J. G. Tobin, B. W. Chung, M. A. Wall, and A. J. Schwartz, Phys. Rev. Lett. **93**, 097401 (2004).

¹⁰K. T. Moore, G. van der Laan, J. G. Tobin, B. W. Chung, M. A. Wall, and A. J. Schwartz, Ultramicroscopy **106**, 097401 (2006).

¹¹G. van der Laan and B. T. Thole, Phys. Rev. B **53**, 14458 (1996).

¹²B. T. Thole and G. van der Laan, Phys. Rev. A **38**, 1943 (1988); Phys. Rev. B **38**, 3158 (1988).

¹³Electron diffraction and imaging of the Am sample in the TEM showed that it contained heavy amounts of stacking faults,

which can be argued produces a combination of α and β phases as it is simply a change in the 111 plane stacking. However, spectra taken from areas with varying amounts of stacking faults showed no detectable difference in branching ratio. Thus, α - and β -Am should have very similar $N_{4,5}$ spectra and, in turn, branching ratios.

¹⁴R. D. Cowan, *The Theory of Atomic Structure and Spectra* (University of California Press, Berkeley, 1981).

¹⁵K. T. Moore, G. van der Laan, R. G. Haire, M. A. Wall, and A. J. Schwartz, Phys. Rev. B **73**, 033109 (2006).

¹⁶K. T. Moore, M. A. Wall, A. J. Schwartz, B. W. Chung, D. K. Shuh, R. K. Schulze, and J. G. Tobin, Phys. Rev. Lett. **90**, 196404 (2003).

¹⁷K. T. Moore, G. van der Laan, R. G. Haire, M. A. Wall, A. J. Schwartz, and P. Söderlind, Phys. Rev. Lett. **98**, 236402 (2007).

¹⁸J. H. Shim, K. Haule, and G. Kotliar, Nature (London) **446**, 513 (2007).

¹⁹J. G. Tobin, P. Söderlind, A. Landa, K. T. Moore, A. J. Schwartz, B. W. Chung, M. A. Wall, J. M. Wills, R. G. Haire, and A. L. Kutepov, Phys. Rev. B (to be published).

²⁰J. C. Lashley, A. Lawson, R. J. McQueeney, and G. H. Lander, Phys. Rev. B **72**, 054416 (2005).

²¹S. K. McCall, M. J. Fluss, B. W. Chung, M. W. McElfresh, D. D. Jackson, and G. F. Chapline, Proc. Natl. Acad. Sci. U.S.A. **103**, 17179 (2006).

²²P. Söderlind and A. Landa, Phys. Rev. B **72**, 024109 (2005).

²³P. Graf, B. B. Cunningham, C. H. Dauben, J. C. Wallmann, D. H. Templeton, and H. Ruben, J. Am. Chem. Soc. **78**, 2350 (1956).